Textures and Microstructures, 1993, Vol. 22, pp. 1–15
Reprints available directly from the publisher.
Photocopying permitted by license only

TEXTURES IN MULTIPHASE MATERIALS
A Review

S. LAZIK AND C. ESLING

Laboratorie de Métallurgie des Matériaux Polycristallins (LM2P), Université de Metz, 57045 Metz, France

(14 May, 1993)

The purpose of this paper is to survey the investigation of textures in multiphase materials. As there is an increasing interest in multiphase materials in such fields as metals, ceramics, polymers and geological materials, efforts were made to overcome the experimental difficulties of texture measurement specific to these materials. Up to now the determination of texture was mostly restricted to two phase materials. Further investigation is necessary to obtain a systematic knowledge about the influence and relationship of the phases involved and to design materials with controlled properties.

KEY WORDS Multiphase materials, texture study.

INTRODUCTION

The first qualititive studies on texture were carried out soon after discovering X-ray diffraction. This method developed quite rapidly eversince. However, when currently manufacturing highly performing texture diffractometers, using new analysing techniques (peak profile analysis) and further developing texture analysis (low symmetry materials, peak separation in the orientation space), major improvements can be achieved. Thus it is currently possible to analyse the texture of materials of complex composition. The requirements imposed on the measuring and analytical procedures have been stepped up as compared to single-phase materials. The latter procedures had to be adapted in several cases.

More recently the fact that new materials should be developed has gained in importance considering that they have to be applied to ever more complex systems.

In the case of a multiphase material each phase may have its own texture. Therefore, the complete texture of such a material consists in the textures of all components considered individually and the correlations between these textures. The multiphase character appears in two ways: through the interaction of neighbouring phases and the transformation of one phase into another.

For example, high strength sheet steels are used increasingly in the automotive industry with a view to improving safety and reducing fuel consumption by weight reduction (Vlad and Bunge, 1981; Mandziej *et al.*, 1984; Costa Viana and Mendonca Brandao, 1984). Intermetallics like Ti–Al compounds with a relatively small specific weight and a relatively high melting point are being developed for extreme conditions i.e. high temperatures, resistance to high variations in

temperature (Mecking, Lütjering and Morii, 1988; Morii *et al.*, 1987). Glass-ceramics consisting of crystallised and amorphous phases as bioactive bone compensation materials, dental materials (medicine), materials with a high resistance to temperature variation (air and space drive), piezoelectric and pyroelectric materials etc. (Bunge, 1990). On the other hand, because of applications in geology, texture analysis has a major role to play for a better understanding of the history of the earth.

RECENT DEVELOPMENTS IN EXPERIMENTAL TECHNIQUES

The measuring of texture can be carried out radiographically, optically or magnetically by several experimental methods. The most important method is X-ray diffraction. Two other methods are based on the same principle: electron and neutron diffraction.

As it is based on the comparatively very low penetration depth of electrons, electron microscopy offers the unique possibility of diffracting from well-defined locations in the sample and high resolution microstructure imaging. X-ray diffraction makes it possible to investigate the local or surface texture—a type of investigation in which statistics play a more important part since the penetration depth is greater than in the case of electrons and the measured area is larger. Owing to the much lower absorption coefficients and therefore the high penetration depth of the neutrons as compared with X-rays, the global or volume texture may thereby be investigated. Comprehensive summaries are provided in Underwood, 1961; Wassermann and Grewen, 1962; Kudrawzew, 1965; Coulomb, 1972; Bunge, 1982; Bunge, 1986; Welch and Puch, 1986 and Schwarzer and Weiland, 1988a.

In the case of multiphase materials, particularly low symmetry crystals characterized by a manifold of reflections with partly high peak overlap, it is sometimes difficult to measure the texture of all existing phases. Table 1 shows examples of some common materials (Brokmeier, 1989).

Figure 1 shows the extreme line-rich neutron diffractogram of a lherzolithe sample (composed of olivine, orthoenstatite, clinoenstatite and some accessory

Table 1 Number of Bragg-reflections for some common materials ($\leq 80°$ in 2ϑ; $\lambda = 0.25$ nm; $d_{min} = 0.1944$ nm), using the Joint Committee on Powder Diffraction Standards (JCPDS) files, (Brokmeier, 1989).

Material	*Phase composition*	*Number of reflections*	*JCPDS*
Al/Pb	two-phase		04-0787
	composite	4	04-0686
Al/Al_2O_3	two-phase		04-0787
	composite	8	10-0173
$TiAl–Ti_3Al$	two-phase		05-0678
	intermetallic	10	14-0451
lherzolithe	three-phase rock		
	-olivine	76	20-1139
	-orthoenstatite		19-0768
	-clinoenstatite		19-0769

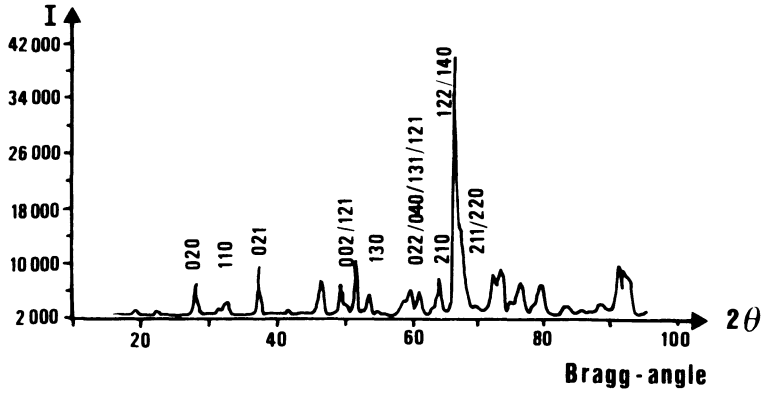

Figure 1 2θ-diagram of a lherzolithe sample, some of the olivine reflections are marked (Brokmeier, 1989).

materials) performed at the Institut Max von Laue–Paul Langevin (ILL) in Grenoble. With such a sample with a high number of partly overlapping Bragg-reflections, it was necessary to have an extended conception for texture measurement:

(1) Optimization of the experimental conditions;

(2) Introduction of the peak profile analysis into texture analysis;

(3) Pole figure inversion with overlapping pole figures (Brokmeier, 1989).

Therefore, special improvements are introduced into the experimental techniques.

Neutron diffractometry paired with position sensitive detector (PSD) technology is a most powerful technique to study patterns of multiphase and low-symmetry materials (Schäfer *et al.*, 1991). Several pole figures can be recorded simultaneously using a PSD (without complex intensity corrections, such as those required in X-ray PSD diffraction technique due to severe geometrical aberrations). PSDs will solve another serious problem, i.e. peak overlap or superposition (Will *et al.*, 1990). This problem is widely encountered for multiphase materials such as rocks or ceramics.

A new method has been developed to determine mineral grain orientations in coarse-grained multiphase materials by single-crystal neutron scattering. The method is based on time-of-flight (TOF) neutron scattering, using a single-crystal diffractometer with a position-sensitive area detector (Schultz and Leung, 1986). In order to accomplish that grain-by-grain orientation neutron diffraction, existing single-crystal orientation techniques used for the TOF neutron single-crystal diffractometer at the Intense Pulsed Neutron Source (IPNS) were modified (Carpenter, Lander and Windsor, 1984).

Furthermore, new computer programs have to be implemented in order to process the large amount of experimental data, measure pole figures with new scanning routines and optimize time and memory space.

It is possible with transmission electron microscopy (TEM) to determine textures of phases with small differences in lattice parameters and orientation

relationships between the grains possibly belonging to different phases, by measuring the orientation of each single grain (Schwarzer and Weiland, 1988a). A semi-automatic method was developed, permitting the computer-assisted on-line measuring of Kikuchi patterns directly from the TEM. In this method, each grain can be selected after one other by focussing the primary beam spot on the area selected to obtain its Kikuchi pattern (convergent beam electron diffraction: CBED) (Schwarzer and Weiland, 1984, 1988b).

CHARACTERISATION OF METALS

Ferrous Materials

A wide variety of textures in dual-phase steels can be developed by metallurgical and thermomechanical processes acting in combination.

In the work by Weiland, Schwarzer and Bunge (1988) a low carbon dual-phase steel (0.05% C, 0.44% Si, 2.55% Mn) with 20 vol.% martensite obtained by cold rolling and intercritical open-coil annealing was studied with TEM before and after a tensile test with 14% elongation.

After intercritical annealing the texture of the ferrite phase (Figure 2a) is similar to the typical recrystallisation texture of low carbon steels. The main component is a fibre deviating 11° from the (111)-fibre. The (110)-fibre typical of iron recrystallisation textures is not well developed. An additional (211) [1–31] component appears in the ODF with the same intensity as the (111)-fibre. The martensite shows only a weak texture (Figure 2b).

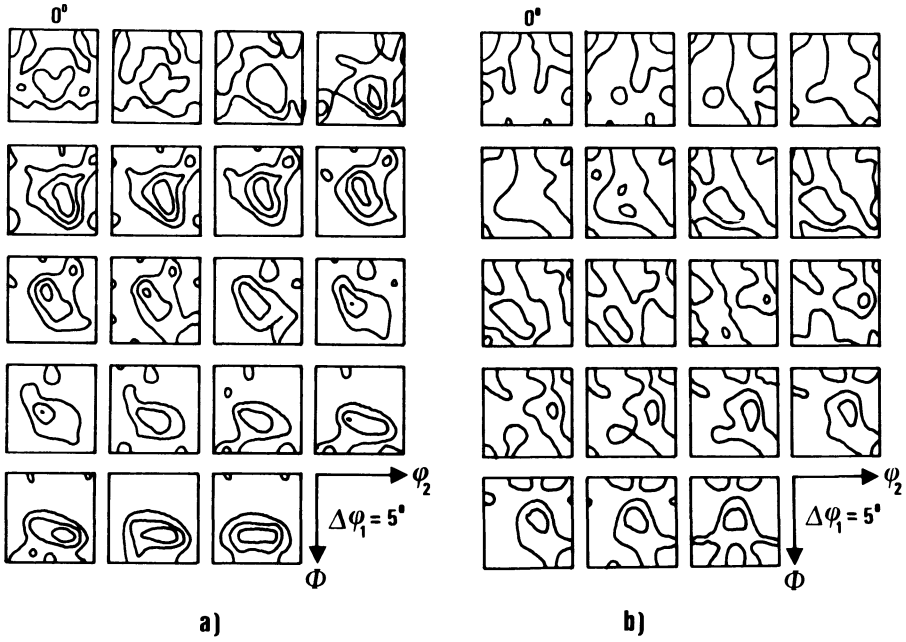

Figure 2 ODF of the ferrite (a) and martensite (b) phase after intercritical annealing, measured by electron diffraction (Weiland *et al.*, 1988).

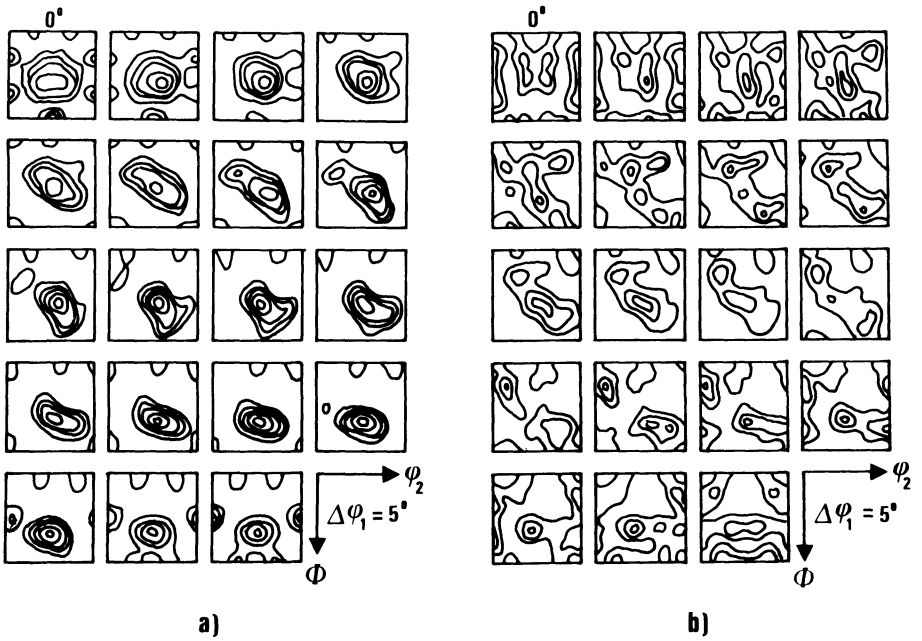

Figure 3 ODF of the ferrite (a) and martensite (b) phase after tensile test by electron diffraction (Weiland *et al.*, 1988).

By the tensile test the textures of both the ferrite and the martensite phases are modified. As shown in Figure 3a in the ferrite texture the main component is shifted 7° towards the (111)-fibre axis. Compared with the nearly random orientation distribution in the inital state, the martensite shows now a well developed texture similar to the typical iron deformation texture (Figure 3b). As with ferrite, the martensite texture consists of a fibre close to (111) and a strong (211) [1–31] component. It may be inferred from this that martensite deforms like ferrite but to a lower degree of deformation.

The fibre textures occurring in microduplex structures of dual-phase (ferritic-austenitic) stainless steel X5CrNiTi26.6 during plastic deformation by tension or compression, especially at temperatures $T \leq 300°K$, were studied with neutron diffraction by Klimanek *et al.* (1984).

After a thermomechanical treatment with hot rolling at over 1100°K to have a metallurgical reference state (austenite content $50 \pm 2\%$) the δ-ferrite shows a rather weak hot-working texture with its main components close to $\langle 110 \rangle$ (deformation texture) and $\langle 100 \rangle$ (recrystallisation texture). The austenite shows a clearly dominating $\langle 100 \rangle$ component (Figure 4a).

The orientation changes occurring in tensile deformation (Figure 4b) can be summarized as follows. Stretching at 77°K causes a rapid decrease of the austenite texture. Simultaneously, in the bcc phase (δ-ferrite, martensite), a well-defined $\langle 110 \rangle$ fibre texture is found even after small elongation (texture inheritance on the base of the Nishiyama-Wassermann relationship (e.g. Jung, 1983) and dislocation slip in the δ-ferrite and martensite). When performing tensile tests at

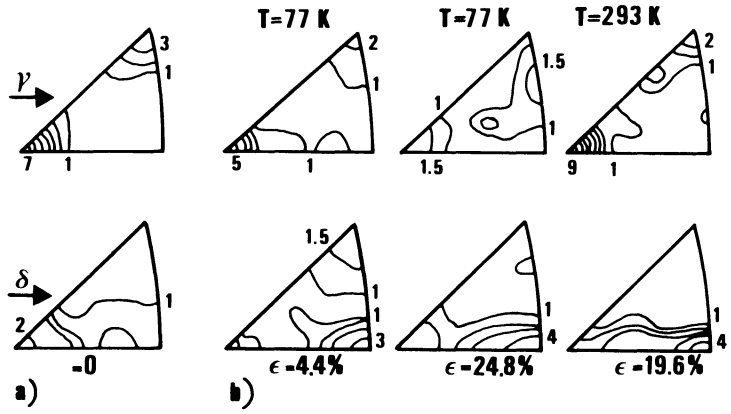

Figure 4 Inverse pole figures of δ-ferrite and austenite before (a) and after (b) tensile deformation at 77 and 293 K (Klimanek *et al.*, 1984).

room-temperature the ⟨100⟩ + ⟨111⟩ double fibre texture of the austenite is well-developed for all degrees of deformation. However, the orientation density of the ⟨100⟩-component increases while the ⟨111⟩-component decreases. A ⟨110⟩-fibre texture is also observed in the bcc phase (δ-ferrite).

Compression at 293°K causes a rapid destruction of the initial austenite texture (a consequence of mechanical twinning and martensite formation) (Figure 5); this also applies to steching at 77°K or cold-rolling at room temperature (Klimanek, Mücklich and Hennig, 1981; Klimanek *et al.*, 1983). In parallel, a ⟨110⟩-compression texture (Wassermann and Grewen, 1962, Hu, 1974), is found in the fcc phase, even after higher strains. In the bcc phase, a ⟨111⟩-fibre texture is formed (Wassermann and Grewen, 1962; Hu, 1974) already at low strain values. A ⟨100⟩-fibre component is found too, whereas the ⟨111⟩-texture dominates at higher strains.

Hot-rolling textures of low carbon dual-phase steels were investigated in the work by Vlad and Bunge (1981) in relation to chemical composition and/or processing parameters, this also applies to the mechanical properties as a function of the prevailing texture. Furthermore, mechanical properties were investigated with respect to texture in the work by Matsuda and Kawashima (1981), Mandziej *et al.* (1984) and Costa Viana and Mendonca Brandao (1984).

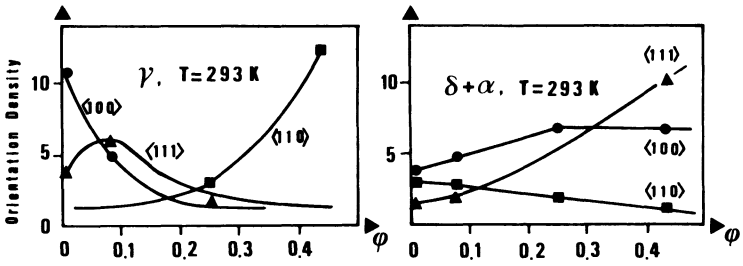

Figure 5 Orientation density changes of the main texture components ⟨uvw⟩ occurring in compression tests at 293 K (Klimanek *et al.*, 1984).

The study of an octahedric iron meteorite sample consisting of bcc kamacite (α-Fe, Ni) and fcc taenite (γ-Fe, Ni) described in the work by Schäfer, Höfler and Will (1988) is of great interest, not only for meteorite research, but also in metallurgy. The orientation relationship between the two phases was analysed according to Kurdjumov–Sachs and Nishiyama–Wassermann α-γ orientations. Martensitic transformation for the α-γ iron phases develops by a process of diffusion controlled nucleation and growth at extremely slow cooling rates.

Non-Ferrous Materials

Dual-phase Ti-6Al-4V alloys with an equiaxial $\alpha + \beta$ microstructure were investigated by Morii *et al.* (1988). To obtain the initial state for the investigating procedure the following heat treatment was applied: annealing at 960°C for 1 h, cooling at about 2°C/min, maintaining at 800°C for 1 h and finally water quenching. Then two samples were rolled in different directions—longitudinal and transversal—to the slab axis up to about 75% reduction at 800°C.

Figure 6 shows the pole figures before and after the subsequent rolling. Both the initial α and β textures turn out to be very weak. The samples have quite different textures in α depending on the direction of the subsequent rolling. The α-texture found in sample I rolled parallel to the longitudinal axis of the slab is

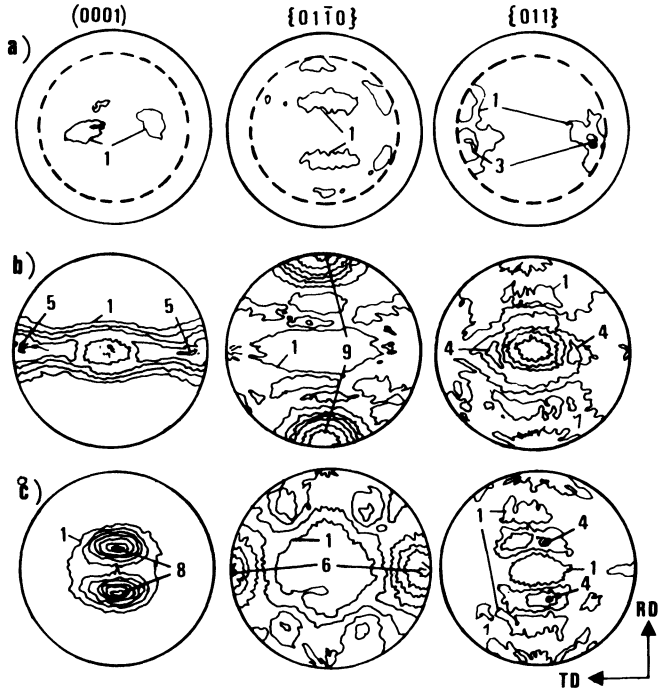

Figure 6 Texture of Ti–6Al–4V alloy rolled to 74% at 800°C. (a) initial texture, (b) specimen I, rolled parallel to the longitudinal axis of the slab, (c) specimen II, rolled parallel to the transverse axis of the slab (Morii *et al.*, 1988).

typical of Ti–6Al–4V alloys rolled in the 700°C–800°C range. The texture in the sample II rolled parallel to the transverse axis of the slab is usually found in cross rolled dual-phase Ti alloys with higher β-volume fraction (ca. 15%) and single phase α-alloys. In contrast to the α-phase the texture of the β-phase was similar for both samples. However, the texture of sample II seems to be weaker than that of sample I.

The evolution of texture in these alloys is closely connected to the sensitivity of microstructural characteristics to the actual parameters of thermomechanical processing such as variation of the temperature of the thermomechanical treatment or the cooling rate. In the work by Mecking, Lütjering and Morii (1988) the effects of microstructural features such as shape, distribution and volume fraction of the α- and the β-parts were explained on slip modes and texture formation in two-phase Ti–6Al–4V.

Multiphase metallic fibre composite sheets, prepared by hot extrusion of precompacted mixtures of carbonyl-iron powder and silver powder with 0, 10, 20 and 30 vol.% Ag were extruded at 800°C to bars (94% reduction) and subsequently cold rolled transverse to the extrusion direction (70% reduction) and then rolled parallel to the extrusing direction (98% reduction), as reported in the work by Welch, Ratke and Wassermann (1984). Whereas the iron texture will be described in each case as a limited fibre texture starting on (100)⟨110⟩ (Schläfer and Bunge, 1974), silver shows a weak modified cube texture in samples at 10 and 30% silver contents (Figure 7). The Kurdjumov–Sachs relationship between iron and silver was discussed; it was also observed in Fe–Cu composites of this type. Under the rolling conditions applied, pure silver developed a completely different texture. It can therefore be assumed that the deformation of silver in the composite is being controlled by the iron matrix.

The textures of the two phases of Al–Pb composite samples of various compositions prepared from powders by 96%-extrusion at room temperature were determined by neutron diffraction by Brokmeier, Böcker and Bunge (1988).

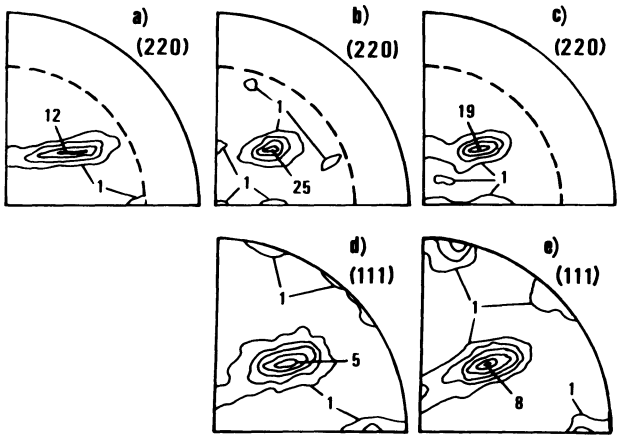

Figure 7 Textures developed in iron-silver composites after extrusion and cold rolling 92%: (a) Pure iron, (b) Fe-10% Ag, (c) Fe–30% Ag, (d) Fe–10% Ag (silver), (e) Fe-30% Ag (silver); (Welch *et al.*, 1984).

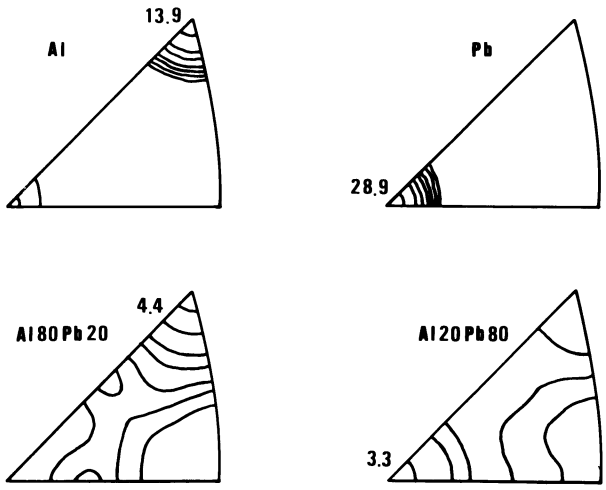

Figure 8 Inverse pole figures of the pure metals and of the Al and Pb-phase of Al–Pb composites deformed 96% by extrusion at room temperature (Brokmeier *et al.*, 1988).

Inverse pole figures of the pure metals and of two composites are given in Figure 8. It can be seen that pure Al develops a strong ⟨111⟩-deformation texture with only a minor ⟨100⟩-component, whereas pure Pb develops a strong ⟨100⟩-recrystallisation texture. The textures of the composites are much weaker but contain the same two texture components. In each phase the sharpness of texture decreases as the volume fraction of the other phase increases. In the case of the harder Al-phase this is due to the decreasing degree of internal deformation of the hard Al-particles in the soft Pb-matrix (Figure 9a). In the case of the softer Pb-phase the decrease must be related to increasing turbulence of flow in the soft phase. Furthermore, this phase was recrystallized after extrusion, cf. Böcker, Brokmeier and Bunge (1988), Brokmeier, Böcker and Bunge (1988).

The deformation texture was studied by Ratke, Seifert and Wassermann (1984) and Böcker, Brokmeier and Bunge (1988) for cold extruded Al–Cu composites. Some examples of calculated inverse pole figures are given in Figure 10. It can be seen that the harder Cu phase has developed a strong ⟨111⟩-deformation texture with only a minor ⟨100⟩-component. As with Al–Pb the texture of the harder phase Cu is sharpening with increasing volume fraction. This reinforcement can be attributed to the increasing degree of the internal deformation in the harder phase when increasing the volume fraction (Figure 9b).

Texture changes in cold extruded and subsequently heat treated Al–Cu composites were investigated up to 400°C by Gertel, Brokmeier and Bunge (1993). It was observed that the recrystallisation textures of both Cu and Al differ, although the lattice structure is the same. The deformation texture of Al is stable for whatever heat treatment, whereas the Cu texture decreases drastically from 300°C upwards. Because of the reduced Cu texture component, multiple twin formation reinforces a tendency towards random texture during recrystallization. The recrystallisation texture also depends on the stacking fault energy.

Ratke, Seifert and Wassermann (1984) found that the Cu texture in Al–Cu

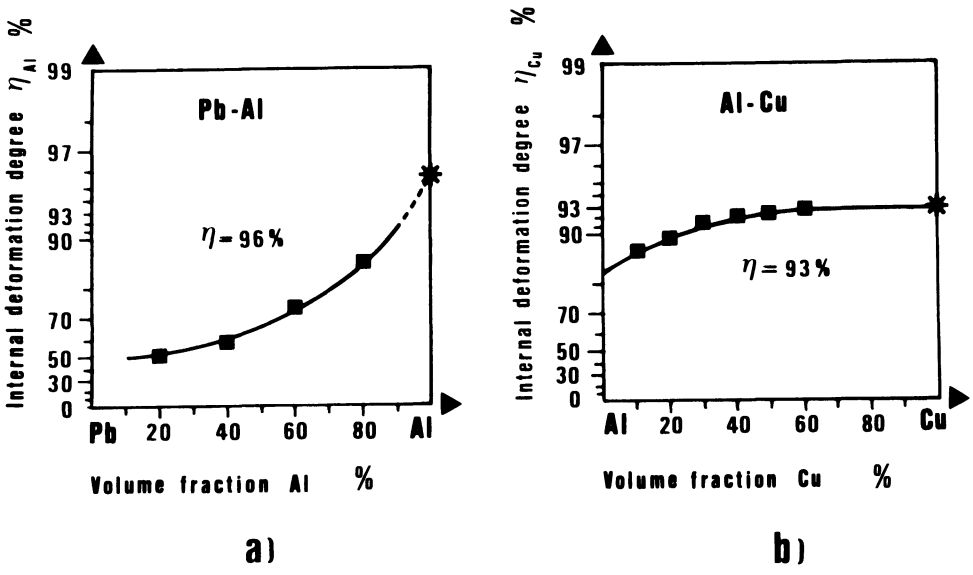

Figure 9 (a) The internal deformation degree of Al-fibres in Pb–Al composites as a function of the volume fraction of Al (Böcker *et al.*, 1988). (b) The internal deformation degree of Cu–fibres in Al–Cu composites as a function of the volume fraction of Cu (Böcker *et al.*, 1988).

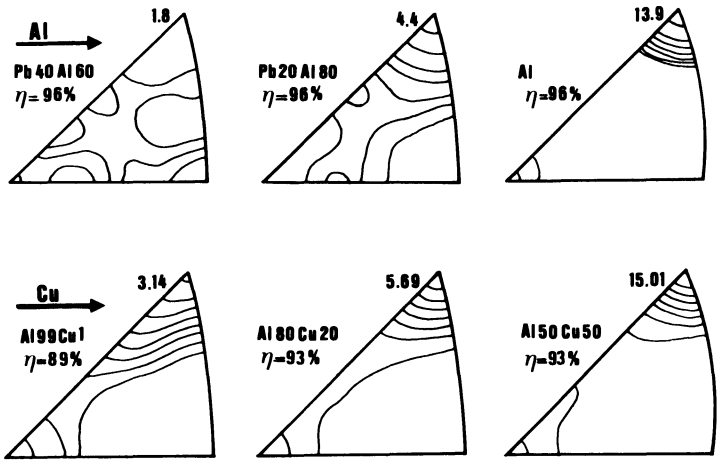

Figure 10 Inverse pole figures of the harder phases Al and Cu in Pb–Al and Al–Cu composites respectively (Böcker *et al.*, 1988).

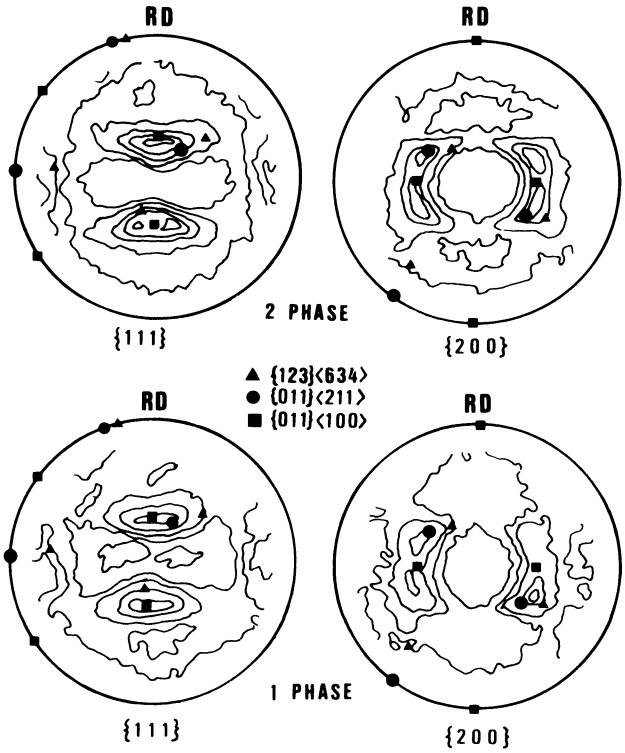

Figure 11 Rolling textures of aged and supersaturated Cu5% Ag (Kim, Gottstein, 1988).

samples, deformed up to 93%, with 20, 40 and 60 vol.% Cu is always the same. This suggests that the Cu content has no influence on the Cu texture. However, such behaviour of the Cu phase could not be confirmed in the work by Gertel, Brokmeier and Bunge (1993).

Heavily rolled (95% thickness reduction) supersaturated single phase and aged (at 600°C) dual-phase Cu 5% Ag were investigated in the work by Kim and Gottstein (1988). The rolling textures of both materials shown in Figure 11 are typical transition type rolling textures, consisting essentially of brass $\{011\}\langle 211\rangle$ and Goss $[011]\langle 100\rangle$ orientation, but also with an intensity close to the S-orientation $\{123\}\langle 634\rangle$ and, to a minor extent, to the Cu orientation $\{112\}\langle 111\rangle$.

The recrystallization texture of the two-phase material is essentially a retained deformation texture (transition type rolling texture) comprising Goss, Brass and S orientation as well as a minor Cu component. Hence, the recrystallization process of the two-phase alloy can be considered as recrystallization in situ, i.e. essentially a recovery process without major nucleation and growth of new recrystallized grains.

CHARACTERISATION OF NON-METALLIC MATERIALS

Crystallographic orientations of individual mineral grains were determined in two samples of mantle eclogite from South African kimberlites (Roberts–Victor) in the work by Smyth, Vergamini and Schultz (1988) by single-crystal neutron scattering. Eclogites are composed primarily of garnet (cubic) and clinopyroxene (monoclinic). The large unit cell of garnet (160 atoms) and the low symmetry of the pyroxene cause peak overlap problems. Typical grain sizes are in the range of 1 to 10 mm. For each grain, the Eulerian cradle setting angles to bring the (100) plane to diffracting condition were computed and then the cell constants, azimuth and dip for each major axis ([100], [010] and [001]) were calculated. The pole figures were calculated and contoured (Figure 12) from these data on grains.

Significant preferred orientations occur in both samples of the cubic garnet and monocline clinopyroxene. They appear to be consistently oriented with respect to the observed grain-shape foliation of the rock. The more coarse-grained and less foliated sample (SRV-4) shows the stronger preferred orientation in both garnet

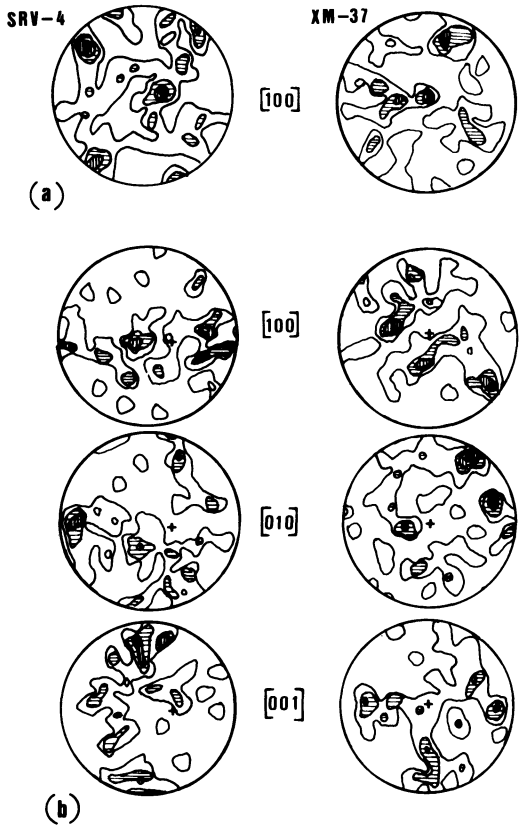

Figure 12 Contoured lower-hemisphere equal-area projection plots of the (a) garnet crystallographic axes [100] and (b) clinopyroxene crystallographic axes [100], [010], [001] for both samples. An approximate pole to the plane of the sample foliation is indicated (+), (Smyth *et al.*, 1988).

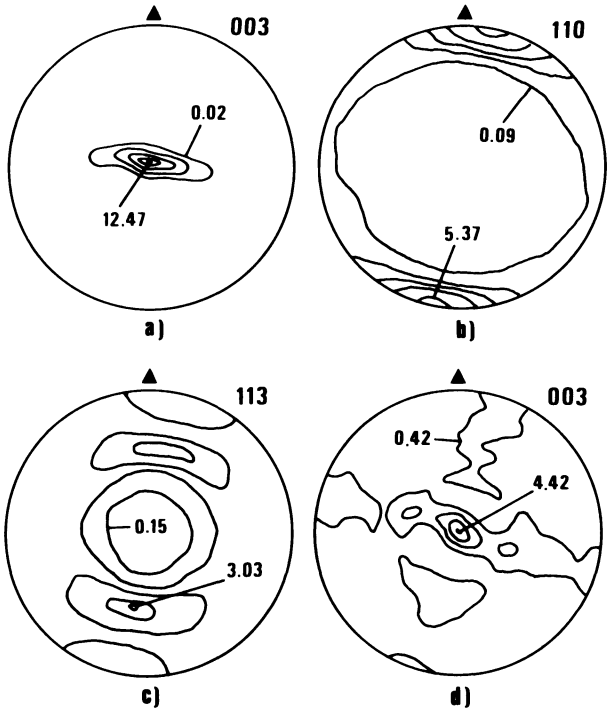

Figure 13 Calculated pole figures from the integrated intensities after profile analysis of all individual diagrams, (a)–(c) Hematite, (d) Biotite, (Will *et al.*, 1990).

and clinopyroxene. The consistent correlation of preferred orientation with foliation indicates that the most likely cause of both features is tectonic deformation (Smyth, Vergamini and Schultz, 1988).

A two-phase hematite ore consisting of hematite and biotite (about 5 vol.%), was investigated by Will *et al.* (1990) with a PSD (Schäfer *et al.*, 1991). Some of the pole figures are shown in Figure 13. It can be seen that a strong texture occurs in both phases, hematite and biotite. The pole figures of both hematite and biotite reveal a strong preferred orientation with central c-poles, which is interpreted by the authors as an inverse fibre diagram.

CONCLUSIONS

Bibliographical research was carried out to provide an overview about recent results and developments in multiphase material texture analysis.

In relation to the purpose of the study and of the materials of interest, various experimental techniques were applied. In general, the existing literature is confined to two-phase materials; moreover, in several cases, the investigation was restricted to only one of the two phases.

The real properties of materials are influenced by all phases. It is therefore necessary to conclude on the relationships between each other. The study of only

one phase does not allow to draw conclusions about the whole set of the properties of materials.

Additional information can be obtained by considering the orientation correlation between the actual phases (misorientation distribution functions), e.g. for a detailed understanding of deformation, recrystallisation and grain growth.

The current state of texture analysis allows to explain specific properties on the basis of a study of two-phase materials. Further investigation will be necessary to obtain a systematic knowledge of the relationships between various phases and their interaction to elaborate property controlled materials.

References

Böcker, W., Brokmeier, H. G. and Bunge, H. J. (1988). Neutron diffraction determination of texture development in two-phase alloys. *Proc. of ICOTOM 8*, J. S. Kallend and G. Gottstein eds., The Metallurgical Society, Inc., Santa Fe, USA, 959–964.

Brokmeier, H. G. (1989). Neutron diffraction texture analysis of multi-phase systems. *Textures and Microstructures* **10,** 325–346.

Brokmeier, H. G., Böcker, W. and Bunge, H. J. (1988). Neutron diffraction texture analysis in extruded Al–Pb composites. *Textures and Microstructures* **8 & 9,** 429–441.

Bunge, H. J. (1982). *Texture Analysis in Material Science.* Butterworths Publ., London.

Bunge, H. J. (1986). *Experimental Methods of Texture Analysis.* DGM Informations gesellschaft Oberursel, H. J. Bunge ed.

Bunge, H. J. (1990). Textur und Anisotropie kristalliner Stoffe. *Sonderforschungsbericht* 1984. TU Clausthal, Germany.

Carpenter, J. M., Lander, G. H. and Windsor, C. G. (1984). Instrumentation at pulsed neutron sources. *Review of Scientific Instruments* **55,** 1019–1043.

Costa Viana, da C. S. and Mendonca Brandao, L. P. (1984). Texture and formability of a dual-phase Al-killed steel. *Proc. of ICOTOM 7,* C. M. Brakman, P. Jongenburger and E. J. Mittemeijer eds., Netherland Society for Materials Science, Zwijndrecht, The Netherlands, 581–584.

Coulomb, P. (1972). Les textures dans les métaux de réseau cubique. Dunod, Paris.

Gertel, H., Brokmeier, H. G. and Bunge, H. J. (1993). Texture development in extruded Al–Cu composites. *Textures and Microstructures,* to be published.

Hu Hsun (1974). *Texture* **1,** 233.

Jung, G. V. (1983). *J. Appl. Cryst.* **16,** 535.

Kim, W., Gottstein, G. (1988). Texture and microstructure in single and two phase Cu 5% Ag. *Proc. of ICOTOM 8,* J. S. Kallend and G. Gottstein eds., The Metallurgical Society, Inc., Santa Fe, USA, 649–660.

Klimanek, P., Betzl, M., Hötzsch, G., Matthies, S. and Mücklich, A. (1984). Fibre textures in low-temperature deformation of two-phase stainless steel X5CrNiTi26.6. *Proc. of ICOTOM 7,* C. M. Brakman, P. Jongenburger and E. J. Mittemeijer eds., Netherlands Society for Materials Science, Zwijndrecht, The Netherlands, 333–338.

Klimanek, P., Mücklich, A. and Hennig, K. (1981). Neutron-diffraction studies of texture changes due to cold-rolling of two-phase stainless steel X5CrNiTi26.6. *Proc. of ICOTOM 6,* S. Nagashima ed., The Iron and Steel Institute of Japan, Tokyo, Japan, 901–909.

Klimanek, P., Scherke, R., Hennig, K. and Mücklich, A. (1983). *Proc. 4th Int. Symposium on Metallurgy and Materials Science,* Risö, 339.

Kudrawzew, J. P. (1965). Textures in metals and alloys (russ). *Metallurgia,* Moscow.

Mandziej, S., Verbraak, C. A., Beyer, J. and Kolster, B. H. (1984). Texture and anisotropic behaviour of dual-phase steel. *Proc. of ICOTOM 7,* C. M. Brakman, P. Jongenburger and E. J. Mittemeijer eds., Netherlands Society for Materials Science, Zwijndrecht, The Netherlands, 421–426.

Matsuda, S. and Kawashima, Y. (1981). Mechanism of separation of a low-carbon low alloy steel controlled rolled at austenite and ferrite two phase regions. *Proc. of ICOTOM 6,* S. Nagashima ed., The Iron and Steel Institute of Japan, Tokyo, Japan, 659–668.

Mecking, H., Lütjering, G. and Morii, K. (1988). Influence of microstructural anisotropy on deformation texture in two phase Ti–6Al–4V. In: *Directional Properties of Materials,* H. J. Bunge ed., DGM Informationsgesellschaft mbH Verlag, Oberursel, Germany, 239–250.

Morii, K., Hartig, C., Mecking, H., Nakayama, Y. and Lütjering, G. (1988). Deformation modes and texture formation in two phase Ti–6Al–4V alloys. *Proc. of ICOTOM 8,* J. S. Kallend and G. Gottstein eds., The Metallurgical Society, Inc., Santa Fe, USA, 991–996.

Ratke, L., Seifert, R. and Wassermann, G. (1984). Faserverbunddrähte aus Al und Cu ohne intermetallische Phasen. *Zeitschrift für Metallkunde* **75,** 903–910.

Schäfer, W., Höfler, S. and Will, G. (1988). Applications of neutron diffraction pole figure measurements on polycrystalline and monocrystalline metallic samples. Examples from the four-circle neutron diffractometer in Jülich. *Textures and Microstructures* **8 & 9,** 457–466.

Schäfer, W., Merz, P., Jansen, E. and Will, G. (1991). Neutron diffraction texture analysis of multi-phase and low-symmetry materials using the position-sensitive detector JULIOS and peak deconvolution methods. *Proc. of ICOTOM 9,* R. Penelle and C. Esling eds., Societe Francaise de Metallurgie et de Materiaux, Special Issue *Textures and Microstructures* **14–18,** 65–71.

Schläfer, D. and Bunge, H. J. (1974). The development of the rolling texture of iron determined by neutron-diffraction. *Texture,* **1,** 157–171.

Schultz, A. J. and Leung, P. C. W. (1986). Analysis of spallation time-of-flight (TOF) neutron data from a 2-D position-sensitive detector. *Journal de Physique* (Les Ulis, Fr.) **47,** C5, 137–142.

Schwarzer, R. A., Weiland, H. (1984). On-line computerized evaluation of Kikuchi patterns for the determination of preferred orientations and orientation correlations. *Proc. of ICOTOM 7,* C. M. Brakman, P. Jongenburger and E. J. Mittemeijer eds., Netherlands Society for Materials Science, Zwijndrecht, The Netherlands, 839–843.

Schwarzer, R. A. and Weiland, H. (1988a). Texture analysis by the measurement of individual grain orientations—electron microscopical methods and application on dual-phase steel. *Textures and Microstructures* **8 & 9,** 551–577.

Schwarzer, R. A. and Weiland, H. (1988b). Measurement of local textures by electron diffraction-comparison with X-ray texture analysis-. *Proc. of ICOTOM 8,* J. S. Kallend and G. Gottstein eds., The Metallurgical Society, Inc., Santa Fe, USA, 203–208.

Smyth, J. R., Vergamini, P. J. and Schultz, A. J. (1988). Texture analysis in coarse-grained multi-phase rocks by neutron single-crystal diffraction. *Proc. of ICOTOM 8,* J. S. Kallend and G. Gottstein eds., The Metallurgical Society, Inc., Santa Fe, USA, 801–809.

Underwood, F. A. (1961). Textures in metal sheets. Mac Donald, London.

Vlad, C. M. and Bunge, H. J. (1981). The orientation distribution of crystallites in hot rolled dual phase steels and its relationship to the mechanical properties. *Proc. of ICOTOM 6,* S. Nagashima ed., The Iron and Steel Institute of Japan, Tokyo, Japan, 649–658.

Wassermann, G. and Grewen, J. (1962). Texturen metallischer Werkstoffe. 2. *Auflage.* Springer-Verlag, Berlin//Göttingen/Heidelberg.

Weiland, H., Schwarzer, R. A. and Bunge, H. J. (1988). The textures of ferrite and martensite in a dual-phase steel-measured separately by electron diffraction-. *Proc. of ICOTOM 8,* J. S. Kallend and G. Gottstein eds., The Metallurgical Society, Inc., Santa Fe, USA, 953–958.

Welch, P. I. and Puch, K. H. (1986). Practical considerations in the measurement of textures. In: *Quantitative Textures Analysis,* H. J. Bunge and C. Esling eds., DGM Informationsgesellschaft mbH Verlag, Oberursel, Germany, 505–524.

Welch, P. I., Ratke, L. and Wassermann, G. (1984). The effect of deformation on Young's modulus in iron-silver sheet composites. *Proc. of ICOTOM 7,* C. M. Brakman, P. Jongenburger and E. J. Mittemeijer eds., Netherlands Society for Materials Science, Zwijndrecht, The Netherlands, 675–680.

Will, G., Merz, P., Schäfer, W. and Dahms, M. (1990). Application of position sensitive detectors for neutron diffraction texture analysis of hematite ore. *Advances in X-Ray Analysis* **33,** 277–283.